Optogenetic and pharmacological suppression of spatial clusters of face neurons reveal their causal role in face gender discrimination

Arash Afraz[a,b,1], Edward S. Boyden[a,b,c,d], and James J. DiCarlo[a,b]

Departments of [a]Brain and Cognitive Sciences and [c]Biological Engineering, [b]McGovern Institute for Brain Research, and [d]MIT Media Laboratory, Massachusetts Institute of Technology, Cambridge, MA 02139

Edited by David J. Heeger, New York University, New York, NY, and approved March 27, 2015 (received for review December 8, 2014)

Neurons that respond more to images of faces over nonface objects were identified in the inferior temporal (IT) cortex of primates three decades ago. Although it is hypothesized that perceptual discrimination between faces depends on the neural activity of IT subregions enriched with "face neurons," such a causal link has not been directly established. Here, using optogenetic and pharmacological methods, we reversibly suppressed the neural activity in small subregions of IT cortex of macaque monkeys performing a facial gender-discrimination task. Each type of intervention independently demonstrated that suppression of IT subregions enriched in face neurons induced a contralateral deficit in face gender-discrimination behavior. The same neural suppression of other IT subregions produced no detectable change in behavior. These results establish a causal link between the neural activity in IT face neuron subregions and face gender-discrimination behavior. Also, the demonstration that brief neural suppression of specific spatial subregions of IT induces behavioral effects opens the door for applying the technical advantages of optogenetics to a systematic attack on the causal relationship between IT cortex and high-level visual perception.

object recognition | face | gender discrimination | optogenetics | inferior temporal cortex

Face neurons in the inferior temporal (IT) cortex are classically defined as all neurons whose responses discriminate visual images of faces from images of nonface objects (1). By the spirit of this definition, an ideal "face neuron" would be a unit that responds to any image containing a face and does not respond to any image containing only nonface objects. Such a hypothetical face neuron could, in principle, directly support face-detection behavior (detecting images of faces with various poses, sizes, positions, and identities among other stimuli) but is not necessarily useful for other face-related behaviors such as face discrimination (distinguishing two different faces). Thus, the mechanistic relationship between "face (detector) neurons" and other face-related behaviors remains far from clear.

Although previous human neuropsychology (2–4), transcranial magnetic stimulation (TMS) (5, 6), and electrophysiological (7, 8) work motivates the hypothesis that face (detector) neurons are causally involved in face discrimination, there is little direct evidence for it. In this study, we aimed to test this hypothesis for one face-discrimination task: Is face gender* discrimination impaired by temporary silencing of IT subregions enriched with face (detector) neurons? Because distributed IT cortical populations show the computational capacity to support a wide range of invariant object discriminations (9, 10)[†], the main alternative hypothesis we considered is that discrimination of different faces (i.e., different objects) can be causally supported by IT neurons outside of the face-detector neural clusters. Beyond this specific scientific question, our study was also motivated by the larger goal of developing better tools for direct manipulation of high-level visual neural activity in primates. That is, although "correlational" analysis of patterns of neural activity can strongly infer a role for those neurons in supporting a behavior, the most direct way to test the "causal" role of the spiking activity of a subset of neurons in a given behavioral task is to directly perturb that neuronal activity and measure its effect on the behavior (11, 12).

Previously, direct electrical perturbation of specific IT subregions had been used to show the causal role of face-detector neurons in face-detection behavior (12), a result that is consistent with the current operational definition of those neurons. Although anecdotal studies in humans reported perceptual distortion of faces after electrical stimulation of large parts of fusiform cortex in humans (13–15), and TMS studies revealed the impact of large-scale perturbation of functional MRI (fMRI)-defined face-selective cortical regions (16) in face recognition (5, 17), a direct causal link between spiking of IT face neurons and face-discrimination behavior has not been established.

In this study, using standard electrophysiology techniques in macaque monkeys and the traditional operational definition of face (detector) neurons, we recorded extensively from central IT cortex (CIT) (18) to locate the largest known spatial cluster of face neurons (also known as middle face patch) (ref. 19; see *SI Methods* for more details). Then, using optogenetic tools, we directly suppressed the spiking activity of ∼1-mm (Fig. S1) subregions of IT cortex enriched with face-detector neurons as well as other nearby

Significance

There exist subregions of the primate brain that contain neurons that respond more to images of faces over other objects. These subregions are thought to support face-detection and discrimination behaviors. Although the role of these areas in telling faces from other objects is supported by direct evidence, their causal role in distinguishing faces from each other lacks direct experimental evidence. Using optogenetics, here we reveal their causal role in face-discrimination behavior and provide a mechanistic explanation for the process. This study is the first documentation of behavioral effects of optogenetic intervention in primate object-recognition behavior. The methods developed here facilitate the usage of the technical advantages of optogenetics for future studies of high-level vision.

Author contributions: A.A. and J.J.D. designed research; A.A. performed research; A.A. and E.S.B. contributed new reagents/analytic tools; A.A. and J.J.D. analyzed data; A.A. and J.J.D. wrote the paper; and E.S.B. contributed with tool development.

Conflict of interest statement: E.S.B. is an inventor on multiple patents covering optogenetic tools.

This article is a PNAS Direct Submission.

Freely available online through the PNAS open access option.

[1]To whom correspondence should be addressed. Email: afraz@mit.edu.

This article contains supporting information online at www.pnas.org/lookup/suppl/doi:10.1073/pnas.1423328112/-/DCSupplemental.

*Following the conventions of the field, the word "gender" here refers to the difference in the visual appearance of male and female faces. We are aware that "sex" is a better descriptor of this physical difference in contemporary English.

[†]Majaj NJHH, Solomon EA, DiCarlo JJ, Computation and Systems Neuroscience (COSYNE), February 23–26, Salt Lake City, UT.

IT subregions and assessed the causal contribution of each subregion in face gender-discrimination behavior.

In a separate set of experiments, using pharmacological intervention (muscimol microinjection), we aimed to replicate our main optogenetic findings. Although the lower spatial resolution and much lower temporal resolution of pharmacological tools does not allow fine comparison of small IT subregions (as is possible with optogenetics), its bigger spatial impact (~3-mm diameter) was used to confirm the basic characteristics of our main finding with a well-established neural suppression method.

Results

We trained two macaque monkeys (*Macaca mulatta*) on two tasks: (*i*) a fixation task (Fig. 1*A*) and (*ii*) a face gender-discrimination task in which they used one of two eye movements to indicate the gender of a briefly presented image of a face (Fig. 1*B*). The visual stimuli were presented parafoveally to the left or right of the fixation point for both tasks (*SI Methods*). To minimize the possibility that the gender-discrimination task might be performed based on low-level cues, such as luminance or local shape cues, or be based on memorization of specific training images, we varied the luminance and shape of the faces in each gender group (Fig. 1*C*) and used a large image set (*SI Methods*). We also confirmed that each animal could generalize the training to new sets of images (performance was >90% for both animals the first time they were presented with new image sets).

After training, we recorded from 353 sites across IT cortex (150 sites in the left hemisphere of monkey C and 203 sites in the right hemisphere of monkey E; *SI Methods*) and determined the multiunit selectivity profile at each site by using a standard rapid serial visual presentation (RSVP) paradigm during the fixation task (Fig. 1*A*). Following the conventions of previous work (12), we measured the d′ of the multiunit spiking response for distinguishing images of faces from images of nonface objects presented in the fixation task, and we defined face-detector units as all those with a face detection d′ (FD) > 1. Face-detection index was defined for each recording penetration as the average neural FD of all multiunits recorded in superior temporal sulcus (STS) along the penetration track. A high FD penetration track was defined as having face-detection index greater than (or equal to) 1, and a low FD penetration track was defined as having face-detection index < 1. We stereotactically located a large (~3 × 4 mm) spatial cluster of high FD neurons in the lower bank of the STS in both monkeys that, based on stereotaxic location, is likely to be the mediolateral (ML) "middle face patch" reported in earlier fMRI (19) and physiology (20, 21) reports.

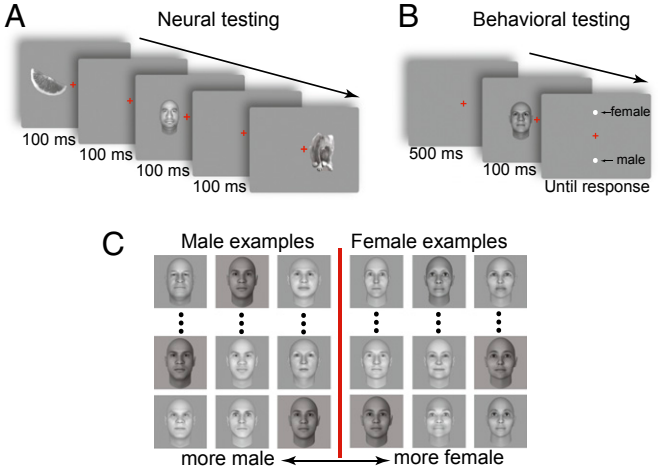

Fig. 1. Behavioral tasks and stimuli. (*A*) Passive fixation task. For neural response testing, each animal maintained fixation at the center of the display while images of faces, bodies, and other objects were presented 20 times in random order in an RSVP paradigm. The objects were restricted in an imaginary ~4° x 6° window and presented at 2.15° to the left or right of the center of gaze. (*B*) Face gender-discrimination task. In each trial, the animals fixated on a central spot for 500 ms, then a stimulus appeared to the left or right of the fixation point (2.15° eccentricity) for 100 ms, followed by two response targets. To receive reward, the animals had to make a saccade to one of the two fixed response targets to report the facial gender of the stimulus. (*C*) The stimulus set for the gender-discrimination task included 400 grayscale computer-generated faces (FaceGen; 18 are shown here). The visual appearance (age, race, and other structural features) of the stimuli varied in each group (see examples), but the morphing "gender signal" (horizontal axis) was held at a level to keep the animal at 85–95% correct.

Optogenetic Neural Suppression. For optogenetic neural perturbation, we injected Adeno Associated Virus 8 (AAV-8) engineered to express ArchT (a neural hyperpolarizing agent) (22) in all infected neurons. We made a single viral injection in the STS at the border of the high FD neural cluster and its neighboring cortex (*SI Methods*). This injection was done to transduce the virus in both high FD subregions and nearby low FD subregions with minimal tissue damage. Earlier histological work following a similar virus injection in the STS of another monkey showed that AAV-8 expression spreads several millimeters around the injection site (Fig. 2*A*), consistent with our ability to optogenetically suppress neural activity at IT subregions at least 2.2 mm away from the injection site.

Optogenetic experimental sessions started 1 month after viral injection. In each experimental session ($n = 40$ sessions), a custom-made optrode was used to first measure the spiking selectivity and the photosensitivity at each of two or three multiunit IT sites during a simple fixation task (*SI Methods*). Photosensitivity was measured by using a 200-ms-duration laser pulse (Fig. 2*B*) delivered to the recording site through the fiber optic on randomly selected presentations of a preferred visual image for each site (*SI Methods*). Next, the optrode was repositioned so that the tip of the optical fiber was at the top of the STS (±500 μm) and kept at this position for the remainder of the session. The monkey was then cued to perform the face gender-discrimination task, during which the same 200-ms laser pulse was delivered on half of the behavioral trials, pseudorandomly selected (each animal typically completed ~1,600 behavioral trials per session).

We tested photosensitivity of 108 IT sites over 16 cortical subregions, all within a 4.4-mm-diameter region of IT centered on the viral injection site in each monkey. A total of 58 of the 108 sites (53.7%) showed significant laser-induced decrease in spiking activity (t test, $P < 0.01$), whereas no sites showed a significant increase. Fig. 2 summarizes the optogenetic effect on the responses of the 99 IT sites (of 108) that expressed visually evoked activity (defined as having above-baseline activity 50–250 ms after image onset without laser). Among these sites, the median optogenetic effect was a suppression of 33% of the visually evoked spikes; Fig. 2 includes an example of such a site. However, consistent with previous work (23), we observed a wide range of optogenetic effects (Fig. 2*C*), ranging from no significant photosuppression to strong photosuppression below background firing (>100% of evoked spikes deleted; Fig. 2*C*). The distributions of optogenetic neural inactivation (Fig. 2*C*) were indistinguishable in the two animals [Kolmogorov–Smirnov (KS) test, $P = 0.27$].

Optogenetically Induced Behavioral Effects. To first ask about the potential causal role of high-FD IT neurons in face discrimination, we examined changes in behavioral performance resulting from photosuppression applied at high-FD IT neural sites (Fig. 3). We found that photosuppression at high-FD sites ($n = 17$ sites) produced, on average, a small but highly significant [mean = 2.02%, median = 1.8%, $t(16) = 5.99$, $P < 0.0001$] drop in behavioral performance in the contralateral visual field (VF) (Fig. 3*A*). This

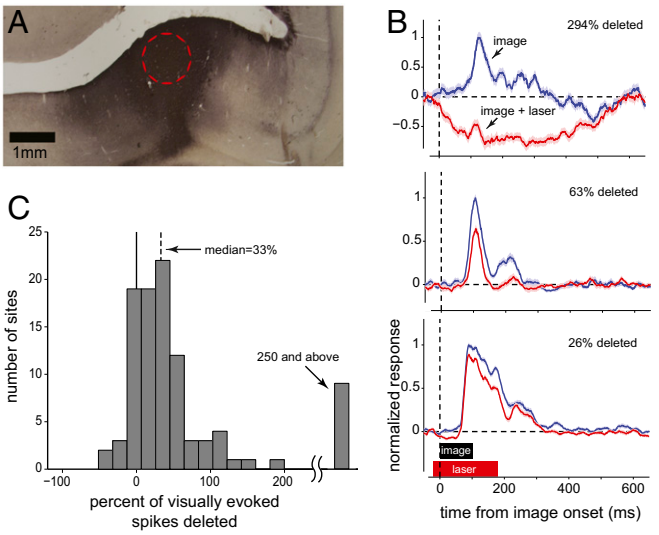

Fig. 2. Neural effects of optogenetic perturbation of the IT cortex. (*A*) Virus transduction zone. A section of monkey STS transduced (~8 months before euthanasia) with AAV-delivered ArchT–GFP, stained with anti-GFP antibody (dark region), is shown. The dashed circle shows the size of the estimated effective suppression zone for a single optical fiber. (*B*) Examples of optogenetic neural suppression observed at different sites in the IT cortex. Blue lines show multiunit response (median of 60 repeated presentations) to the site's preferred image (100 ms; black bar) obtained during RSVP. Red lines show mean response to the same visual image, but with the laser light also delivered to the site (200-ms duration; red bar). Laser-on presentations were randomly interleaved with regular image presentations. Pink and light-blue shadings show ±1 SE. The numbers next to each subplot indicate percentage of visually evoked spikes deleted by light (with respect to the site's baseline spiking rate; dashed line). (*C*) Distribution of optogenetic suppression of all visually driven IT sites that were tested for light sensitivity ($n = 99$). Percent of visually evoked spikes deleted is defined as 100 x $(R - R_L)/R$, where R is the baseline subtracted multiunit response to the preferred stimulus (50- to 250-ms temporal window), and R_L is the same with laser on.

effect was significant for each monkey separately ($P < 0.02$ for both monkeys; see Fig. S2 for the data presented separately for the two animals). We also found that photosuppression applied at these high-FD sites produced no significant change in face-discrimination performance for faces presented in the ipsilateral VF [mean = −0.96%, median = −1.35%, $t(16) = -1.92$, $P = 0.07$]. This lack of a detectable average behavioral effect for the ipsilateral VF is consistent with the well-known contralateral preference of IT neurons (24–27), which we confirmed within our own recordings (ipsilaterally evoked response was only 45% of contralaterally evoked response for the preferred stimulus; $n = 353$ sites).

To test the possibility that the laser-induced neural suppression and behavioral reduction (high-FD neural sites, contralateral VF) was due not to light-gated channels, but to some other effect of tissue illumination (e.g., heating effects), we also performed 12 experimental sessions at high-FD neural sites before viral injection in one of the animals. No significant neural or behavioral effects of cortical illumination were observed, even with comparable statistical power (Fig. 3*B*).

To compare the causal role of high- and low-FD neurons, we next looked at the behavioral effect of photosuppression of IT sites with low face selectivity ($n = 23$ sites with mean FD < 1). We found that photosuppression at these IT sites produced, on average, no significant effect on performance for faces presented in either the contralateral [mean = 0.35%, median = 0.25%, $t(22) = 0.89$, $P = 0.38$] or the ipsilateral VF [mean = 0.05%, median = 0.25%, $t(22) = 0.16$, $P = 0.9$]. Importantly, this lack of effect cannot be simply explained by a failure to photosuppress neurons at the low FD sites, because the distributions of photosuppression over low- and high-FD sites were indistinguishable (KS test, $P = 0.33$).

To determine whether these results reflect a true change in perceptual gender discriminability (d′) or a change in the animals' choice biases, we calculated the behavioral d′ and the decision criterion (C) for each condition. We found that the results expressed in units of d′ largely mirrored those expressed as percent correct. Photosuppression at high-FD sites produced a significant drop [mean = 0.19, median = 0.17, $t(16) = 6$, $P < 0.0001$] in behavioral d′ in the contralateral VF, but not the ipsilateral VF [mean = −0.1, median = −0.11, $t(16) = -1.9177$, $P = 0.07$]. No effect of photosuppression on behavioral d′ was observed for low-FD sites, neither for the contralateral [mean = 0.06, median = 0.06, $t(21) = 1.5381$, $P = 0.14$] nor for ipsilateral VF [mean = 0.01, median = 0.02, $t(21) = 0.2014$, $P = 0.84$]. We found no evidence of any significant change in the animals' decision criterion (choice bias) across different conditions. Fig. S3 summarizes this analysis.

Rather than simply lumping the IT sites into two groups (low and high FD; above), we plotted the FD against the change in behavioral performance across all 40 experimental sessions. Consistent with the results in Fig. 3*A*, we found a significant negative correlation for stimuli presented to the contralateral VF ($r = -0.46$, $P < 0.01$; Fig. 3*C*; the correlation remains significant for the data collected from each animal: $r = -0.73$, $P < 0.01$ and $r = -0.56$, $P < 0.05$ for monkeys C and E, respectively) but not for the ipsilateral

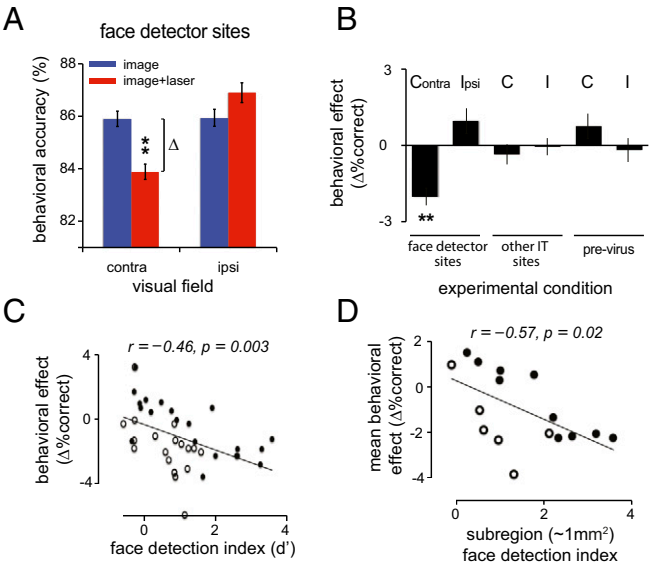

Fig. 3. Behavioral effects of optogenetic suppression of local IT neural activity. (*A*) Face-detector sites. Shown is the mean behavioral effect of photosuppression applied at high-FD cortical sites (penetrations with face-detection index > 1). The ordinate shows the behavioral accuracy of the animals on the gender-discrimination task. The abscissa indicates the VF in which the stimulus was presented. All four trial types were randomly interleaved. (*B*) The behavioral effect of cortical illumination for various experimental conditions tested for images presented in the contralateral (C) and ipsilateral (I) VF. The ordinate depicts the behavioral effect (change in the behavioral accuracy for the gender-discrimination task; see *A*). Face-detector sites, summarizes the data already shown in *A*; other IT sites, same for low-FD sites (face-detection index < 1) with equivalent neural suppression (see text); pre-virus, same for high-FD IT sites before viral injection. Error bars show ±1 SE. $^{**}P < 0.01$. (*C*) Behavioral effect of photosuppression for all experimental sessions after the viral injection. The abscissa shows the face-detection index of the targeted site. The ordinate indicates the photo-induced behavioral effect for contralaterally presented images. Each data point shows an experiment session. (*D*) Behavioral effect of photosuppression pooled for small (~1 mm^2) subregions of IT cortex (see text). In *C* and *D*, open and closed circles depict the data from monkeys E and C, respectively.

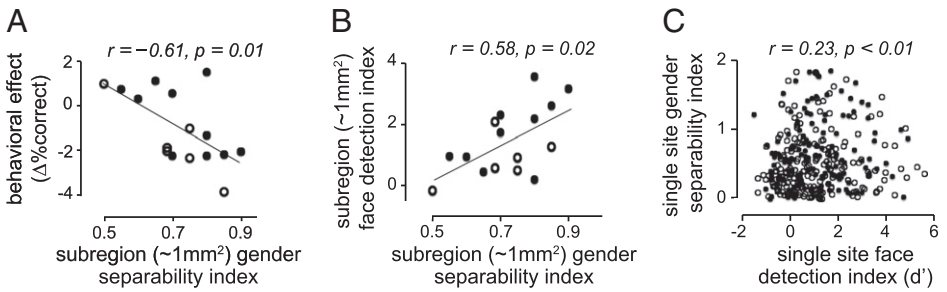

Fig. 4. Explicit encoding of facial gender in CIT. (*A*) The relationship between explicit neural encoding of facial gender in various IT subregions and the effect of photosuppression of those subregions on face gender-discrimination behavior. The abscissa shows, for each IT subregion, the gender classification performance of a linear classifier trained and tested (independent image presentations) on all sites collected within that subregion (*SI Methods*). The ordinate shows the average impact of photosuppression of those subregions (pooled across multiple sessions) on the animals' gender-discrimination performance for contralaterally presented images. (*B*) The relationship between explicit neural encoding of facial gender and average face-detection index (FD) over all tested IT subregions. The abscissa is the same as *A*. The ordinate shows the mean neural FD (d') for all of the neurons recorded from each cortical subregion. (*C*) The relationship between neural encoding of facial gender and FD in all recorded IT sites (not pooled). The abscissa represents FD for all individual sites recorded in IT cortex, and the ordinate represents separability of the gender signal (defined as absolute d′ of the multiunit response for separating male and female stimuli) in the same sites ($n = 353$). Seven data points with ordinate values > 2 or abscissa values > 6 are not shown here for illustration purposes. Open and closed circles represent monkeys E and C, respectively.

VF ($r = 0.074$, $P = 0.65$; absolute $r < 0.2$ and $P > 0.5$ in both animals). Linear regression suggests that suppression of sites with no face-detection signal (FD = 0) had, on average, a −0.27% impact on performance, whereas sites with the highest observed face-detection signal (mean FD ~ 3.6) produced a −3.1% impact.

The analyses above are presented as if neural activity at single IT sites should be predictive of the behavioral impact of illumination applied at that site. However, because our optogenetic protocol is expected to impact all neurons within a ~1-mm diameter spherical region emanating from the optical fiber tip (23), those initial analyses are likely too simplistic because they do not attempt to account for this 1-mm spread. Thus, we next sought to summarize the degree of neural face selectivity in each optically targeted IT subregion by computing the mean FD of all neural sites recorded within each of the ~1-mm^2 subregions tested (i.e., 16 recording grid locations; median of nine sites recorded at each location; *SI Methods*). We found that 8 of the 16 IT subregions had mean FD > 1.0, consistent with previous reports of strong spatial clustering of single neurons with high FD (12, 20, 21). We then plotted the average photo-induced change in the animals' behavioral performance as a function of the mean FD of each tested IT subregion. The former was computed by averaging the change in behavioral performance observed over all experimental sessions performed at that subregion (median of two sessions). Consistent with the earlier analyses, these measures were significantly negatively correlated for faces presented to the contralateral VF ($r = −0.57$, $P = 0.02$) (Fig. 3*D*) but not for the ipsilateral VF ($r = 0.36$, $P = 0.17$).

As described in the Introduction, a commonly accepted hypothesis is that high-FD subregions in the IT cortex are causally involved in supporting all face-related tasks (28). The results above provide support for this hypothesis in at least one such task (face gender discrimination). However, this hypothesis is not satisfying in that it does not offer any computational explanation of why face-detector neurons should support face discrimination. Thus, we considered a different, computationally motivated hypothesis: Every object-related task depends only on the IT subregions that convey explicit (i.e., linearly decodable) information about that task. For instance, under this hypothesis, our face gender-discrimination task depends on the IT subregions that express the most explicit information about gender and does not rely on other IT subregions. This hypothesis predicts that photosuppression of any "explicit gender information" in IT subregions will produce the strongest behavioral impact, regardless of their ability to support face-detection task (*Discussion*). To test this prediction, we measured the amount of explicit information (cross-validated linear separability; *SI Methods*) about our face gender task in each of the tested IT subregions and plotted that against each subregion's average photo-induced change in behavioral performance (computed exactly as in Fig. 3*D*). This analysis revealed that, over the 16 IT subregions, the amount of explicit information for face gender strongly predicted the contralateral behavioral deficit resulting from photosuppression of that subregion ($r = −0.6$, $P = 0.01$) (Fig. 4*A*).

Pharmacological Suppression. We next aimed to compare the behavioral effects produced by optogenetic methods with those produced by a well-established pharmacological neural suppression method (muscimol microinjection) that has less spatial resolution and at least four orders of magnitude less temporal resolution (23, 29) (*SI Methods*). In six experimental sessions, we stereotactically targeted the center of the high-FD neural cluster (in both monkeys) for muscimol microinjection (*SI Methods*). We used microinjectrodes (30) to record the neural activity before muscimol injection, to measure the FD of each targeted IT subregion, and to precisely execute small microinjections along the entire cortical thickness.

We found that injection of muscimol in high-FD subregions of IT cortex resulted in a significant drop in face gender-discrimination performance only for faces presented in the contralateral VF, whereas performance remained unchanged in the ipsilateral hemifield [Fig. 5*A*; repeated-measures ANOVA interaction test, $F(4,20)=7.5$, $P < 0.001$]. Sliding paired t test (including all sessions) showed a significant drop in performance for the contralateral presentations compared with the ipsilateral presentations for all behavioral blocks taken 30 min after muscimol injection [$t(5) > 3.9$; $P < 0.007$, Bonferroni corrected for all, 5.53% performance difference between the ipsilateral and contralateral VFs averaged for all data points collected after an hour from the end of microinjection; Fig. 5*B*]. We also performed six experimental sessions injecting muscimol at neighboring IT loci (at least 2 mm away from the closest recorded high-FD subregion), and we found no detectable behavioral impact on the face-discrimination task [repeated-measures ANOVA interaction test, $F(4,20)=1.7$, $P = 0.18$]. The pattern of results was similar for both animals (Fig. S4). In addition, we performed two experimental sessions injecting saline (1 μL) into high-FD subregions and found no detectable behavioral effect (Fig. 5*B*).

Discussion

Here we used neural suppression tools to test the causal link between neural activity in IT subregions enriched with face (detector) neurons and one type of face-discrimination behavior. We found that neural suppression of these high-FD IT subregions produced, on average, a small, but highly significant, reduction in behavioral performance (for contralaterally presented images). In contrast, we were unable to detect any average behavioral impact of neural suppression of other IT subregions. These findings were independently obtained by using both optogenetic and pharmacological neural suppression tools.

NEUROSCIENCE

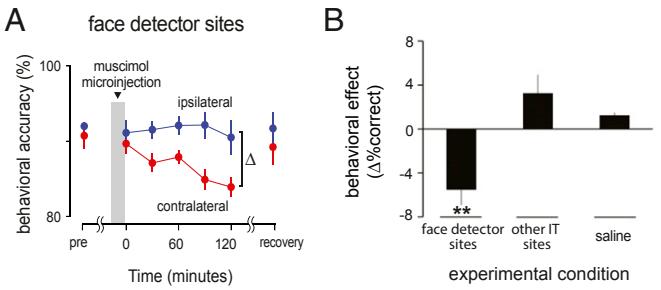

Fig. 5. Behavioral effect of drug microinjection in IT cortex. (*A*) Face-detector sites. The effect of muscimol injection centered over a high-FD subregion of IT cortex on gender-discrimination performance is shown. The ordinate represents the animals' mean behavioral accuracy for the gender-discrimination task. The abscissa represents time. The gray band indicates the duration of muscimol microinjection. The red and blue lines show the behavioral performance for contralaterally and ipsilaterally presented images, respectively. (*B*) Behavioral effect of drug microinjection for various experimental conditions. The ordinate depicts the difference of behavioral accuracy between the ipsilateral and contralateral VFs averaged for all data points collected after 1 h from the end of microinjection. Face-detector sites, summarizes data shown in *A* ($n = 6$ microinjections); other IT sites, microinjections away from high-FD subregions of IT ($n = 6$); saline, microinjection of saline in high-FD subregion ($n = 2$). Error bars show ±1 SE. $^{**}P < 0.01$.

At broad brush, our results (Figs. 3 and 5) provide, to our knowledge, the first direct causal support for the idea that face-related tasks rely preferentially on IT spatial subregions that are enriched with face (detector) neurons (16, 28, 31). Although previous studies have revealed that face-detection signals are not uniformly distributed across the IT cortex, those studies provide little knowledge about the spatial distribution of gender information across the IT cortex. Moreover, knowledge of this spatial distribution would not necessarily dictate the distribution of the causal impact of different IT subregions on the gender-discrimination task. Thus, in the face of these unknowns, the null hypothesis (H0) is that all IT subregions—including high- and low-FD subregions—equally support gender-discrimination behavior. Our results reject this null hypothesis (H0). Assuming that face (detector) neuron clusters in the monkey have homology with regions identified in human fMRI [fusiform face area and occipital face area (OFA)] (31, 32), then our results are consistent with human reports of deficits in face discrimination after damage to human fusiform cortex (2, 3, 33) or after temporary disruption of OFA (5, 17).

Besides rejection of the hypothesis (H0) stated above, what other scientific inferences about neural face processing might we draw from our findings? Tsao and Livingstone (28) proposed that face processing is a two-stage mechanism that involves separate and sequential "detection" and "discrimination" stages. According to that hypothesis (here termed H1), face-detector neurons (mostly concentrated in the middle face patch), without explicitly encoding the differences between classes of faces, serve as a "domain-specific gate" for a later discrimination stage that happens at higher processing stages (e.g., more anterior face patches) (28). This hypothesis (H1) predicts that face-detector neurons, even without explicit encoding of facial gender, contribute causally to face gender discrimination because their activity is required to "gate" the processing of face gender. Our neural suppression results are consistent with this prediction. However, analysis of our neurophysiological data shows that facial gender is explicitly encoded in high-FD IT subregions in the middle face patches (Fig. 4*B*), a result that looks inconsistent with H1. More importantly, the fact that neural encoding of gender in IT local neural populations is the best predictor of their behavioral impact on gender discrimination (Fig. 4*A*) gives birth to an alternative hypothesis (H2). According to H2, every object-related task depends only on the IT neurons that contain explicit (linearly decodable) information about that task (and not on other IT neurons). In the context of face processing, H2 states that, unlike H1, face discrimination is not gated by the activity of face-detection neurons. Instead, H2, more parsimoniously, states that IT neurons that are best at face detection support face-detection behavior, whereas IT neurons that are best at face discrimination support face-discrimination behavior. Our optogenetic and pharmacological neural suppression experiments are consistent with the predictions of H2 (Fig. 4). However, because our neurophysiological data reveal that explicit face gender information is most concentrated in high-FD, millimeter-scale IT subregions (Fig. 4*B*), our neural suppression experiments, considered in isolation, cannot distinguish between H1 and H2. We currently favor H2 because, unlike H1, it is spatially comprehensive (i.e., speaks to all of IT) and task comprehensive (i.e., speaks to all object-related tasks). However, evolution may have settled on special downstream causal linkages for socially important stimuli such as faces, so H1 cannot be dismissed simply because it is less comprehensive.

On a related point, note that H2 (as well as H1) is a specific hypothesis about information readout from the IT cortex. It is absolutely possible to imagine an upstream area (e.g., V1 or V4) that contains information that is not linearly separable, yet its inactivation affects the task performance. The correlation of the behavioral impact of inactivation with linear separability should break down at such an area. The fact that we actually observe a correlation with linear separability in IT cortex suggests that IT representations are relatively close to the mechanisms that drive gender-discrimination behavior and that we have approximated those mechanisms reasonably well with linear decoders.

Are H1 and H2 potentially distinguishable with more spatially precise neural suppression tools? Our data suggest so. Gender and detection information are moderately (Pearson $r = 0.58$), but not perfectly, correlated at the millimeter scale (Fig. 4*B*), suggesting that much larger amounts of data with our current millimeter-scale suppression approach could give more weight to H1 or to H2. Moreover, gender and detection information are only weakly correlated (Pearson $r = 0.25$) at the single site level (Fig. 4*C*), which implies that emerging technology that allows labeling and optogenetic targeting of differently tuned neural populations within cortical subregions (34, 35) should, in principle, allow us to extend our approach to that finer spatial scale.

The behavioral effects of neural suppression reported here are specific in that, for both optogenetic and pharmacological experiments, the effects are limited to the contralateral visual hemifield, and they were not found for other spatial locations in IT where the neural responses were not face selective. However, we have not tested the effect of inactivation of IT neurons in other behavioral tasks. It is possible (and indeed likely if H2 is correct) that face selective parts of IT cortex contribute to tasks that involve discrimination of objects other than faces. Further studies, tailored to study the various task effects, are needed to investigate whether perceptual consequences of suppression of high-FD IT subregions are limited to face-related tasks or they include a wider range of perceptual deficits.

The finding of contralateral task specificity is against the relatively common intuition that retinotopy and even laterality of visual representation decreases dramatically in high-level cortical areas. This common intuition is consistent with large and bilateral receptive fields of IT neurons reported in the classical studies (24, 25) and has led to a lack of visual-field isolation of the stimuli in most of the human neuropsychology studies concerning high-level ventral stream damages (2, 3, 33). Our results, however, clearly demonstrate that IT neurons contribute mainly to visual processing in their contralateral VF. This finding is consistent with more recent estimations of the size of IT receptive fields (26, 27, 36, 37). Although brain plasticity after temporal lobe damage could mask this contralateral bias, rapidly reversible inactivation methods (as used here) are not subject to this limitation.

There have been very few reports of behavioral effects of optogenetic intervention in primate brain (38–40), and induction of such effects has not always been straightforward (41). The present study is, to our knowledge, the first documentation of any behavioral consequence of optogenetic intervention in a high-level ventral stream cortical area in the primate brain. From a technical point of view, the demonstrated utility of optogenetic tools for inducing specific behavioral deficits in face discrimination opens the door for using the technical advantages of optogenetics (e.g., high temporal precision and potential neuronal specificity) for future studies of object recognition and other high-level vision functions. Given that the cortical volume inactivated by 1 μL of muscimol [~3 mm in diameter (29)] is considerably larger than the volume inactivated by a single optical fiber (~1 mm; Fig. S1) (22, 23), we expect the behavioral impact of optogenetics to be smaller than the muscimol-induced effect. Our results are consistent with this intuition (2.0% vs. 5.5% performance change). Although the smaller effect size of optogenetics may be viewed as a disadvantage, we see it as an opportunity, because, given the smaller volume of the cortex inactivated, it allows finer spatial dissection of the role of IT neural populations in visual behaviors. In addition, the high statistical power of optogenetic methods (resulting from trial randomization) allows reliable detection of small behavioral effects.

Another remarkable point about the behavioral effect sizes observed here is that IT is a high-level area in the ventral stream hierarchy. Even massive lesioning or cooling of IT cortex (e.g., removing an entire gyrus) (42–45) leads to behavioral effects smaller (~10–15%) than those after inactivation of early visual areas (46, 47). This finding is consistent with the idea that, in a distributed hierarchical system, inactivation of a low-level cortical subregion that gates incoming information can produce large behavioral effects if behavioral tasks are chosen to isolate that gate. Alternatively, the lack of large behavioral effects after massive lesioning or cooling of IT might have resulted from the use of behavioral tasks that were not chosen to require the processing value added by the ventral stream (e.g., no demand for invariance in the task). Future experiments will hopefully shed more light on such questions.

Methods

All procedures were performed in compliance with standards of Massachusetts Institute of Technology Animal Care and Use Committee. See *SI Methods* for more information.

ACKNOWLEDGMENTS. We thank Kailyn Schmidt for her support throughout the project, Chris Stawarz for code support, Aimei Yang for providing the virus, and Mike Henninger for analysis support. This work was supported by NIH Grants K99 EY022924 (to A.A.), R21 EY023053 (to J.J.D.), and R01 EY14970 (to J.J.D.).

1. Gross CG (2005) Processing the facial image: A brief history. *Am Psychol* 60(8): 755–763.
2. Busigny T, Graf M, Mayer E, Rossion B (2010) Acquired prosopagnosia as a face-specific disorder: Ruling out the general visual similarity account. *Neuropsychologia* 48(7):2051–2067.
3. Susilo T, Duchaine B (2013) Advances in developmental prosopagnosia research. *Curr Opin Neurobiol* 23(3):423–429.
4. Towler J, Eimer M (2012) Electrophysiological studies of face processing in developmental prosopagnosia: Neuropsychological and neurodevelopmental perspectives. *Cogn Neuropsychol* 29(5-6):503–529.
5. Pitcher D, Garrido L, Walsh V, Duchaine BC (2008) Transcranial magnetic stimulation disrupts the perception and embodiment of facial expressions. *J Neurosci* 28(36): 8929–8933.
6. Pitcher D, Walsh V, Duchaine B (2011) The role of the occipital face area in the cortical face perception network. *Exp Brain Res* 209(4):481–493.
7. Rolls ET (1992) Neurophysiological mechanisms underlying face processing within and beyond the temporal cortical visual areas. *Philos Trans R Soc Lond B Biol Sci* 335(1273): 11–20; discussion 20–21.
8. Leopold DA, Bondar IV, Giese MA (2006) Norm-based face encoding by single neurons in the monkey inferotemporal cortex. *Nature* 442(7102):572–575.
9. Hung CP, Kreiman G, Poggio T, DiCarlo JJ (2005) Fast readout of object identity from macaque inferior temporal cortex. *Science* 310(5749):863–866.
10. Rust NC, Dicarlo JJ (2010) Selectivity and tolerance ("invariance") both increase as visual information propagates from cortical area V4 to IT. *J Neurosci* 30(39):12978–12995.
11. Salzman CD, Britten KH, Newsome WT (1990) Cortical microstimulation influences perceptual judgements of motion direction. *Nature* 346(6280):174–177.
12. Afraz SR, Kiani R, Esteky H (2006) Microstimulation of inferotemporal cortex influences face categorization. *Nature* 442(7103):692–695.
13. Allison T, et al. (1994) Face recognition in human extrastriate cortex. *J Neurophysiol* 71(2):821–825.
14. Parvizi J, et al. (2012) Electrical stimulation of human fusiform face-selective regions distorts face perception. *J Neurosci* 32(43):14915–14920.
15. Jonas J, et al. (2014) Self-face hallucination evoked by electrical stimulation of the human brain. *Neurology* 83(4):336–338.
16. Kanwisher N, Yovel G (2006) The fusiform face area: A cortical region specialized for the perception of faces. *Philos Trans R Soc Lond B Biol Sci* 361(1476):2109–2128.
17. Pitcher D, Goldhaber T, Duchaine B, Walsh V, Kanwisher N (2012) Two critical and functionally distinct stages of face and body perception. *J Neurosci* 32(45):15877–15885.
18. Felleman DJ, Van Essen DC (1991) Distributed hierarchical processing in the primate cerebral cortex. *Cereb Cortex* 1(1):1–47.
19. Moeller S, Freiwald WA, Tsao DY (2008) Patches with links: A unified system for processing faces in the macaque temporal lobe. *Science* 320(5881):1355–1359.
20. Tsao DY, Freiwald WA, Tootell RB, Livingstone MS (2006) A cortical region consisting entirely of face-selective cells. *Science* 311(5761):670–674.
21. Issa EB, Papanastassiou AM, DiCarlo JJ (2013) Large-scale, high-resolution neurophysiological maps underlying FMRI of macaque temporal lobe. *J Neurosci* 33(38): 15207–15219.
22. Han X, et al. (2011) A high-light sensitivity optical neural silencer: Development and application to optogenetic control of non-human primate cortex. *Front Syst Neurosci* 5:18.
23. Chow BY, et al. (2010) High-performance genetically targetable optical neural silencing by light-driven proton pumps. *Nature* 463(7277):98–102.
24. Desimone R, Albright TD, Gross CG, Bruce C (1984) Stimulus-selective properties of inferior temporal neurons in the macaque. *J Neurosci* 4(8):2051–2062.
25. Ito M, Tamura H, Fujita I, Tanaka K (1995) Size and position invariance of neuronal responses in monkey inferotemporal cortex. *J Neurophysiol* 73(1):218–226.
26. DiCarlo JJ, Maunsell JH (2003) Anterior inferotemporal neurons of monkeys engaged in object recognition can be highly sensitive to object retinal position. *J Neurophysiol* 89(6):3264–3278.
27. Op De Beeck H, Vogels R (2000) Spatial sensitivity of macaque inferior temporal neurons. *J Comp Neurol* 426(4):505–518.
28. Tsao DY, Livingstone MS (2008) Mechanisms of face perception. *Annu Rev Neurosci* 31:411–437.
29. Arikan R, et al. (2002) A method to measure the effective spread of focally injected muscimol into the central nervous system with electrophysiology and light microscopy. *J Neurosci Methods* 118(1):51–57.
30. Noudoost B, Moore T (2011) A reliable microinjectrode system for use in behaving monkeys. *J Neurosci Methods* 194(2):218–223.
31. Kanwisher N (2000) Domain specificity in face perception. *Nat Neurosci* 3(8):759–763.
32. Grill-Spector K, Knouf N, Kanwisher N (2004) The fusiform face area subserves face perception, not generic within-category identification. *Nat Neurosci* 7(5):555–562.
33. Chatterjee A, Farah MJ (2001) Face module, face network: The cognitive architecture of the brain revealed through studies of face processing. *Neurology* 57(7):1151–1152.
34. Ramirez S, et al. (2013) Creating a false memory in the hippocampus. *Science* 341(6144):387–391.
35. Redondo RL, et al. (2014) Bidirectional switch of the valence associated with a hippocampal contextual memory engram. *Nature* 513(7518):426–430.
36. Afraz SR, Cavanagh P (2008) Retinotopy of the face aftereffect. *Vision Res* 48(1): 42–54.
37. Afraz A, Pashkam MV, Cavanagh P (2010) Spatial heterogeneity in the perception of face and form attributes. *Curr Biol* 20(23):2112–2116.
38. Dai J, Brooks DI, Sheinberg DL (2014) Optogenetic and electrical microstimulation systematically bias visuospatial choice in primates. *Curr Biol* 24(1):63–69.
39. Cavanaugh J, et al. (2012) Optogenetic inactivation modifies monkey visuomotor behavior. *Neuron* 76(5):901–907.
40. Jazayeri M, Lindbloom-Brown Z, Horwitz GD (2012) Saccadic eye movements evoked by optogenetic activation of primate V1. *Nat Neurosci* 15(10):1368–1370.
41. Ohayon S, Grimaldi P, Schweers N, Tsao DY (2013) Saccade modulation by optical and electrical stimulation in the macaque frontal eye field. *J Neurosci* 33(42):16684–16697.
42. Weiskrantz L, Saunders RC (1984) Impairments of visual object transforms in monkeys. *Brain* 107(Pt 4):1033–1072.
43. Horel JA, Pytko-Joiner DE, Voytko ML, Salsbury K (1987) The performance of visual tasks while segments of the inferotemporal cortex are suppressed by cold. *Behav Brain Res* 23(1):29–42.
44. Heywood CA, Cowey A (1992) The role of the 'face-cell' area in the discrimination and recognition of faces by monkeys. *Philos Trans R Soc Lond B Biol Sci* 335(1273):31–37, discussion 37–38.
45. Buckley MJ, Gaffan D, Murray EA (1997) Functional double dissociation between two inferior temporal cortical areas: Perirhinal cortex versus middle temporal gyrus. *J Neurophysiol* 77(2):587–598.
46. Schiller PH, Tehovnik EJ (2008) Visual prosthesis. *Perception* 37(10):1529–1559.
47. Newsome WT, Paré EB (1988) A selective impairment of motion perception following lesions of the middle temporal visual area (MT). *J Neurosci* 8(6):2201–2211.

Supporting Information

Afraz et al. 10.1073/pnas.1423328112

SI Methods

Animals and Surgery. Experiments were performed on two adult male rhesus monkeys (*M. mulatta*). Before behavioral training, aseptic surgery was performed to attach a head post on the skull. After 4–6 months of behavioral training (below), a second surgery was performed to place a recording chamber.

Behavioral Tasks and Visual Images. Stimuli were presented on a video monitor (Acer GD235HZ LCD; 52 × 29 cm, 60 Hz refresh, 1,920 × 1,080 pixels) positioned 40 cm from the monkey so that the display subtended ±33 horizontal and ±20 vertical degree of visual angle. The background luminance of the monitor was 10 cd/m^2; it was the only light source in the room.

Macaque monkeys (*M. mulatta*) were operantly trained on two types of tasks, fixation and face gender discrimination. For the fixation task, each animal was trained to fixate a central dot while visual stimuli were presented in a pseudorandom RSVP sequence (Fig. 1*A*). RSVP images were 60 cutout grayscale pictures of objects, animals, body parts, and faces (30 faces and 30 nonface objects), each sized to just fit in an imaginary 4.3° (h) × 6.4° (v) window. Each image was presented at each of two VF locations—to the left or right of the center of gaze (specifically, with the center of 4.3° × 6.4° imaginary image window located at either −2.15° or +2.15° along the horizontal meridian). Each image presentation was 100 ms in duration, followed by a 100-ms blank period, followed by the next 100-ms image presentation (RSVP). All images (60) and presentation locations (two) were randomly interleaved over the RSVP sequence, and each of these 120 conditions was typically tested 10 times. The animals were given liquid reward for every 2 s of uninterrupted fixation within a 1.5° × 1.5° window, and only neural responses to images presented while the animal was fixating were included in data analyses.

For the face gender-discrimination task, the monkeys were trained to indicate the gender of a briefly presented face by making a saccade to one of the two targets on the screen (Fig. 1*B*). In each trial, the animal fixated at a small fixation point in the middle of the screen for 500 ms. Then a stimulus was presented for 100 ms randomly to the left or right of the fixation (either −2.15° or +2.15° along the horizontal meridian). The animal had to maintain fixation until the stimulus disappeared and two response targets immediately appeared above and below the fixation point (±3.6° along the vertical meridian). The top target was the correct response for female faces and the bottom target was the correct response for male faces, and the monkey received a drop of liquid for making a saccade to the correct target. All of the images used in this task were generated with digital 3D models (FaceGen Modeler; Singular Inversions Inc.), which allow the creation of an infinite number of images for each gender (e.g., infinite number of female faces, varying the face identity and local shape feature randomly, and keeping their femaleness constant). In practice, we first trained the animals on a fixed set of 400 images (200 males and 200 females). The significant variation of the large number of images within each gender was intended to make it impossible for the animal to discriminate between the two genders based on simple low-level features. In addition, because male faces are typically darker and redder than female faces (an easy low-level cue for the animals for performing the task without processing the shape cues), we made all of the stimuli gray scale and varied the luminance of both male and female stimuli substantially (from 8.2 to 24.5 cd/m^2), while keeping the global mean luminance of the two gender groups equal. Also, because all of the stimuli were created based on 3D models, it was possible to morph between the genders to vary the task difficulty of perceptual discrimination between the two genders. Once trained, we tested the animals' performance on freshly generated sets of 400 images to confirm that they could generalize the learning to novel stimuli. As each monkey gained more experience with the task, we occasionally created a new set of 400 images with slightly increased task difficulty to keep the animal's performance level below ceiling (typically between 85–95% correct; chance is 50%). For muscimol experiments, because the test blocks were shorter, smaller image sets (200 images) were used.

Electrophysiology. Conventional recording chambers were implanted on the skull to provide access to the STS and the ventral surface of IT cortex (left hemisphere in monkey C and right hemisphere in monkey E). Multiunit neural responses were recorded using conventional, single-electrode electrophysiology methods (see ref. 1 for details). Before virus injection we recorded extensively from the lower bank of STS and the ventral surface of CIT cortex in the 2- to 9-mm range anterior to the interaural line and located a large (~3 × 4 mm) cluster of face-selective units (defined as FD d′ > 1). Given the anatomical position of the targeted cluster (positioned in the lateral side of the lower bank of STS 5–6 mm anterior to the interaural line) and its large size and high concentration of face-selective neurons (>90% of the recorded units were face-selective), this neural cluster is most likely the same as the ML face patch reported in earlier fMRI (2) and physiology (3, 4) reports.

Optogenetics.

Virus injection. A single viral injection site was selected in each monkey based on earlier stereotactic mapping of the neural selectivity profile of the cortex determined from recordings sampling in the region (above). The border of the face-selective cluster (the lateral border in one monkey and the anterior border in the other animal) in STS was targeted for injection to transduce both a face-selective subregion of IT and its neighboring non-face-selective cortex. Targeting was done based on the stereotactic coordinates and by using a microinjectrode that confirmed neurophysiological properties of the target site before injection (the monkey performed the fixation task, and multiple IT neurons were recorded along the "to be injected" penetration track to confirm the correct positioning of the injection). The targeted cortex was injected with ~6 μL of solution (at 0.1 μL/min rate) containing AAV-8 carrying CAG-ARCHT (5), an outward proton pump with a pan-neuronal promoter (targeting all cell types). Viral titer was ~2 × 10^{12} infectious units per mL. Viral injection procedures are similar to Chow et al. (6).

Optrodes. Each optrode used for the optogenetics experiments was a conventional tungsten electrode glued (5 min epoxy) to a 150-μm diameter optical fiber (numerical aperture 0.22). The tip of the fiber was carefully polished before gluing to the electrode. The tip of optical fiber was typically 0.6–0.9 mm above the tip of the electrode.

Optogenetic experiments. Optogenetic experiments started 4 weeks after the virus injection (the required time for transfection and gene expression). In each experiment session, a custom-made optrode was advanced into the lower bank of STS in a recording track within an STS region 4.4 mm in diameter, centered at the viral injection site. The size of this region was determined based on previous pilot work. Then, the multiunit image selectivity of the recording site was determined by using the RSVP protocol (above). Next, the preferred image of the site was selected for testing the photosensitivity of the multiunit activity. While the

monkey held fixation, the preferred stimulus was presented 40–100 (median = 60) times (as in the RSVP task above, except that a 500-ms blank interval was used between each image presentation). On half of the image presentations (pseudorandomly selected), a 200-ms 532-nm laser impulse (starting from 16.6 ms before the image onset) was delivered to the recording site through the fiber optic (total fiber output power ~12 mW), and the effect of light on the evoked response of the site was evaluated. This procedure (measuring the stimulus selectivity and photosensitivity) was typically repeated for two or three sites along the recording track, and then the optrode was repositioned to place the tip of the optical fiber within ±500 μm of the top of the lower bank of STS. The optrode was kept in this position for the rest of the experimental block, while the monkey—typically—performed 1,600 behavioral trials of the face gender-discrimination task. The laser impulse was delivered to the tissue in random order in half of the trials.

Pharmacological Suppression. For drug injections, handmade microinjectrodes were used based on the design/descriptions presented by Noudoost and Moore (7) to microinject muscimol, a well-known $GABA_A$ agonist, into the cortex. A microinjectrode consists of a platinum-iridium electrode (OD: 80 μm) embedded in a 30-G cannula (OD: 311 μm) connected to a liquid microinjection circuit and conventional electrophysiology equipments. It allowed recording of the neural responses before the injection of drug/virus through the same probe. In each drug injection session, the microinjectrode was advanced to the lower bank of STS, and using the fixation task—similar to optogenetic experiments—the multiunit neural stimulus selectivity was assessed and confirmed. After recording of the neuronal responses along the microinjectrode track, the tip of the microinjectrode was positioned in the middle of the targeted cortex and 1 μL of muscimol (5 mg/mL) was injected at 0.1 μL/min rate. Before and after the muscimol injection, the monkeys performed blocks (400 trials each) of the gender-discrimination task in 30-min intervals (typically total of five blocks).

Linear Classification. Explicit information about face gender in each IT subregion ("linear separability of gender"; Fig. 4*A*) was measured by training a simple Euclidean-distance linear classifier for gender discrimination using the multiunit neural responses (to male and female faces) collected from all neural recordings within the subregion. Data from passive fixation task (RSVP) included neural responses to 10 male and 10 female stimuli sampled from those used in the gender-discrimination task. Using a leave-one-out procedure, we trained the classifier with the neural responses (for all units collected across the different experiment days from each cortical subregion) to 19 images and tested the classification performance on the remaining 1 image, and then we rolled through all of the images and repeated this process. The average performance of the classifier was then correlated with the average behavioral impact of illumination for each cortical track.

1. Rust NC, Dicarlo JJ (2010) Selectivity and tolerance ("invariance") both increase as visual information propagates from cortical area V4 to IT. *J Neurosci* 30(39):12978–12995.
2. Moeller S, Freiwald WA, Tsao DY (2008) Patches with links: A unified system for processing faces in the macaque temporal lobe. *Science* 320(5881):1355–1359.
3. Tsao DY, Freiwald WA, Tootell RB, Livingstone MS (2006) A cortical region consisting entirely of face-selective cells. *Science* 311(5761):670–674.
4. Issa EB, Papanastassiou AM, DiCarlo JJ (2013) Large-scale, high-resolution neurophysiological maps underlying FMRI of macaque temporal lobe. *J Neurosci* 33(38):15207–15219.
5. Han X, et al. (2011) A high-light sensitivity optical neural silencer: Development and application to optogenetic control of non-human primate cortex. *Front Syst Neurosci* 5:18.
6. Chow BY, et al. (2010) High-performance genetically targetable optical neural silencing by light-driven proton pumps. *Nature* 463(7277):98–102.
7. Noudoost B, Moore T (2011) A reliable microinjectrode system for use in behaving monkeys. *J Neurosci Methods* 194(2):218–223.

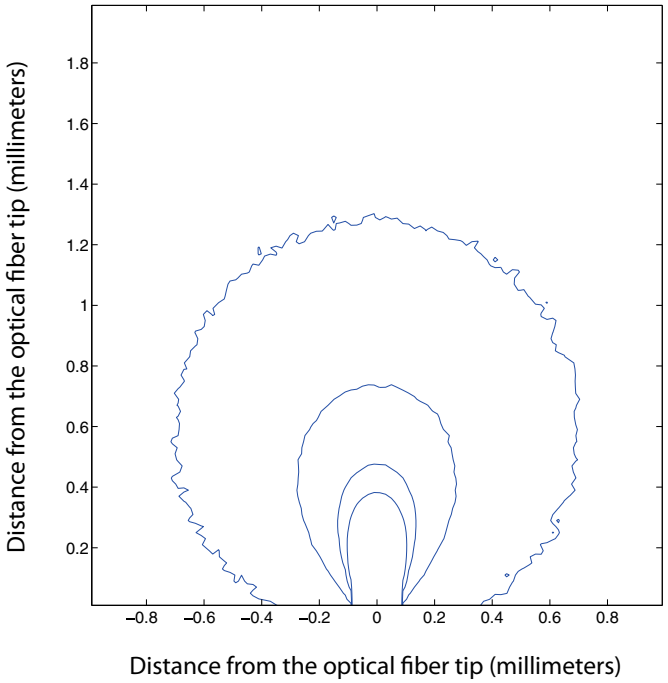

Fig. S1. To estimate the effective spread of the light in the brain tissue, irradiance of the 532-nm green laser in the gray matter is plotted as a function of position relative to the tip of the optical fiber (150-μm diameter, numerical aperture of 0.22, total output power ~12 mW). Laser irradiance was estimated based on the Monte Carlo simulation of light scattering/absorption in the brain tissue. The contours display 100, 10, 5, 2, 1.28, and 1 mW/mm^2 irradiances. For details, please check Chow et al. (6) because a similar procedure is used here.

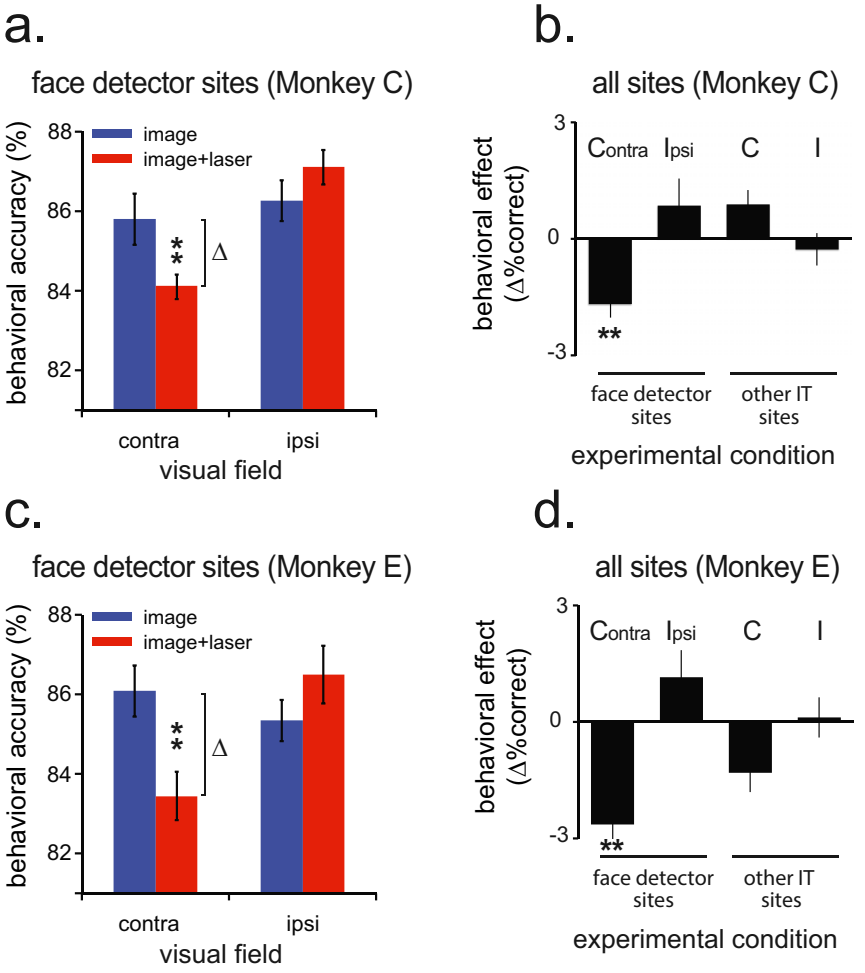

Fig. S2. Behavioral effects of optogenetic suppression of IT activity presented separately for the two animals. All of the axes and definitions are similar to Fig. 3 *A* and *B*. *A* and *B* show the results from monkey C, and *C* and *D* show the results from monkey E. *A* and *C*, face-detector sites; *B* and *D*, all sites. Please note that pre-virus condition (Fig. 3*B*) was tested only for monkey C, and its data are already presented in Fig. 3. $^{**}P < 0.02$.

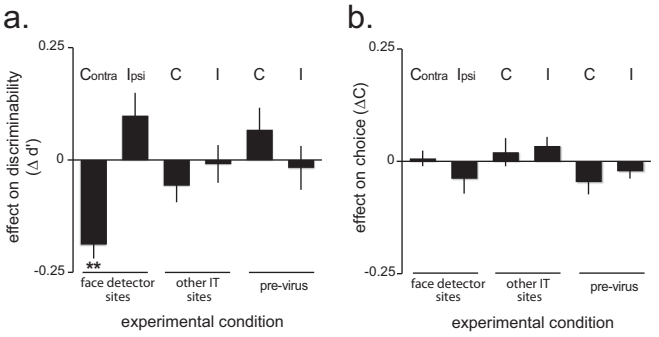

Fig. S3. Effects of optogenetic suppression of IT activity on perceptual gender discriminability and choice bias. (*A*) The effect of cortical illumination on perceptual gender discriminability (behavioral d′) for various experimental conditions tested for images presented in both the contralateral (C) and ipsilateral (I) VF. The panels and axes are similar to Fig. 3*B*. The ordinate depicts the effect of illumination on discriminability (change in the behavioral d′ for the gender-discrimination task). Face-detector sites, summarizes the data already shown in *A*; other IT sites, same for low-FD sites (face-detection index < 1) with equivalent neural suppression (see text); pre-virus, same for high-FD IT sites before viral injection. Error bars show ±1 SE. $^{**}P < 0.01$. (*B*) The axes and conditions are similar to *A* except that the ordinate shows the effect of illumination on the behavioral choice bias (decision criterion).

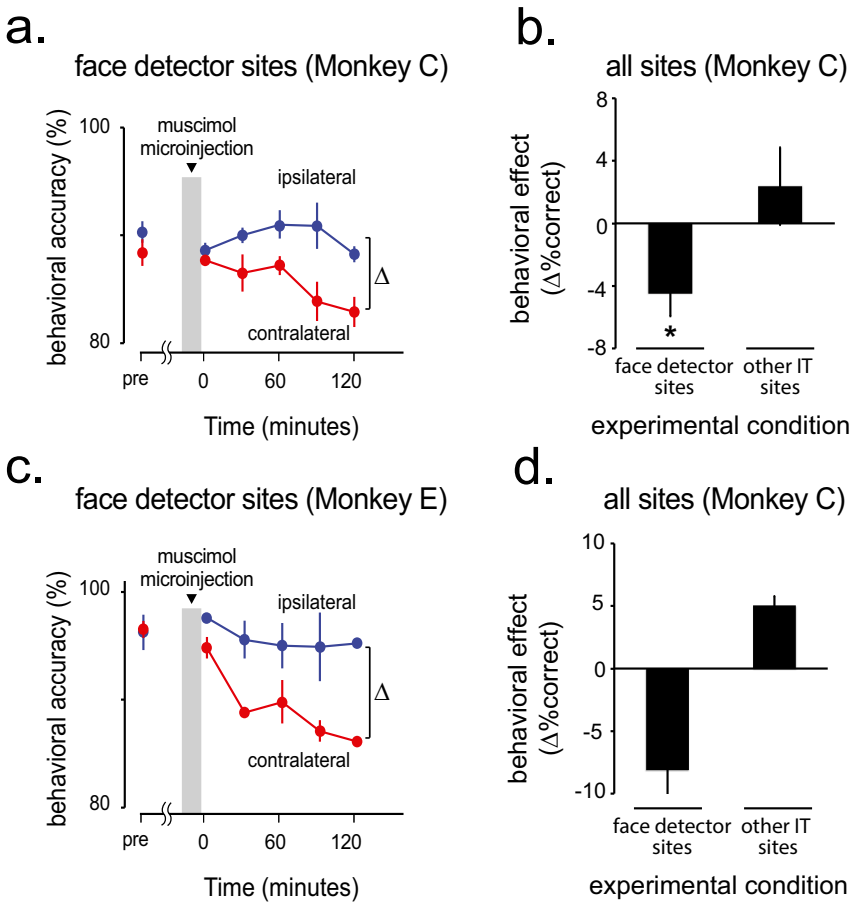

Fig. S4. Behavioral effects of drug microinjection in IT cortex presented separately for the two animals. All of the axes and definitions are similar to Fig. 4 *A* and *B*. *A* and *B* show the results from monkey C, and *C* and *D* show the results from monkey E. *A* and *C*, face-detector sites; *B* and *D*, all sites. Please note that saline condition (Fig. 4*B*) was tested only for monkey C, and its data are already presented in Fig. 4. $*P < 0.05$.